Elsevier Editorial System(tm) for NeuroImage
Manuscript Draft

Manuscript Number: NIMG-13-813R1

Title: On the Use of Cramer Rao Minimum Variance Bounds for the Design of Magnetic Resonance Spectroscopy Experiments

Article Type: Regular Article

Section/Category: Methods & Modelling

Corresponding Author: Dr. Roland Kreis, PhD

Corresponding Author's Institution: University Bern

First Author: Christine S Bolliger, MSc

Order of Authors: Christine S Bolliger, MSc; Chris Boesch, MD,PhD; Roland Kreis, PhD

Abstract: Localized Magnetic Resonance Spectroscopy (MRS) is in widespread use for clinical brain research. Standard acquisition sequences to obtain one-dimensional spectra suffer from substantial overlap of spectral contributions from many metabolites. Therefore, specially tuned editing sequences or two-dimensional acquisition schemes are applied to extend the information content. Tuning specific acquisition parameters allows to make the sequences more efficient or more specific for certain target metabolites. Cramér-Rao bounds have been used in other fields for optimization of experiments and are now shown to be very useful as design criteria for localized MRS sequence optimization. The principle is illustrated for one- and two dimensional MRS, in particular the 2D separation experiment, where the usual restriction to equidistant echo time spacings and equal acquisition times per echo time can be abolished. Particular emphasis is placed on optimizing experiments for quantification of GABA and glutamate. The basic principles are verified by Monte Carlo simulations and in vivo for repeated acquisitions of generalized two-dimensional separation brain spectra obtained from healthy subjects and expanded by bootstrapping for better definition of the quantification uncertainties.

***4. Highlights (for review)**

- Use of Cramer Rao bound criteria to optimize in vivo MR spectroscopy experiments
- Method illustrated for 1D and 2D MRS, in particular 2D separation (2DJ) experiments
- 2DJ generalized to non-equidistant echo times and unequal numbers of scans per TE
- Experiment optimizations discussed for GABA and glutamate as target metabolites
- In vivo verification for sets of human brain spectra expanded by bootstrapping

On the Use of Cramér-Rao Minimum Variance Bounds for the Design of Magnetic Resonance Spectroscopy Experiments

Christine S Bolliger[1], Chris Boesch[1], and Roland Kreis[1]

[1] Institute of Diagnostic, Interventional and Pediatric Radiology, Inselspital, Bern University Hospital, and Department of Clinical Research, University of Bern, Bern, Switzerland

christine.bolliger@insel.ch, chris.boesch@insel.ch, roland.kreis@insel.ch

Corresponding author:

Prof. Dr. sc. nat. Roland Kreis

University Bern,

Inselspital, P.O. Box 35,

CH-3010 Bern, Switzerland

Tel: +41-31-632 8174, Fax: +41-31-632 0580

Email: roland.kreis@insel.ch

Abstract

Localized Magnetic Resonance Spectroscopy (MRS) is in widespread use for clinical brain research. Standard acquisition sequences to obtain one-dimensional spectra suffer from substantial overlap of spectral contributions from many metabolites. Therefore, specially tuned editing sequences or two-dimensional acquisition schemes are applied to extend the information content. Tuning specific acquisition parameters allows to make the sequences more efficient or more specific for certain target metabolites. Cramér-Rao bounds have been used in other fields for optimization of experiments and are now shown to be very useful as design criteria for localized MRS sequence optimization. The principle is illustrated for one- and two dimensional MRS, in particular the 2D separation experiment, where the usual restriction to equidistant echo time spacings and equal acquisition times per echo time can be abolished. Particular emphasis is placed on optimizing experiments for quantification of GABA and glutamate. The basic principles are verified by Monte Carlo simulations and in vivo for repeated acquisitions of generalized two-dimensional separation brain spectra obtained from healthy subjects and expanded by bootstrapping for better definition of the quantification uncertainties.

Keywords

Magnetic Resonance Spectroscopy; Cramér-Rao minimum variance bounds; quantification; experiment optimization; GABA; bootstrapping

1. Introduction

In vivo magnetic resonance spectroscopy (MRS[1]) allows for the in vivo and in situ quantitation of tissue metabolite contents. Different MRS techniques are available and the best suited technique in a particular situation depends on the target metabolites, the organ studied, the (patho-)physiological circumstances, as well as the experimental situation (in particular the B_0 field strength available). Given that metabolite signals in a proton MR spectrum usually have considerable overlap that makes the quantification difficult, generally, one of three different approaches is taken: 1) use of a single non-specific one-dimensional spectrum (e.g. a localized short echo time (TE) spectrum) followed by linear combination model fitting based on prior knowledge about the constituent metabolites and spectral parameters (Provencher, 1993; Ratiney et al., 2005; Slotboom et al., 1998; Wilson et al., 2011), or 2) use of a dedicated (so-called editing) one-dimensional experiment optimized for exclusive or selective sensitivity for a single metabolite of interest, usually followed by simple model peak fitting or signal integration (Allen et al., 1997), or 3) use of a standard localized two-dimensional MR spectrum followed by peak integration (Thomas et al., 1996; Thomas et al., 2001) or prior knowledge fitting (Chong et al., 2011; Gonenc et al., 2010; Kiefer et al., 1998; Kreis et al., 2005; Schulte and Boesiger, 2006; Thomas et al., 2008; van Ormondt et al., 1990; Vanhamme et al., 1999). In cases 1 and 3, the choice of experimental parameters like TE and repetition time (TR) is most often based on general considerations about maximum signal for given relaxation times, insensitivity to changes in relaxation times or arguments about minimization of macromolecular baseline contributions, while in case 2 the signal yield of wanted and unwanted metabolites and their relative overlap is modeled based on quantum mechanical simulations or solution measurements.

---

[1] Abbreviations used:

2DJ:	2D-J separation	Cr:	creatine
CRBs:	Cramér-Rao minimum variance bounds	FiTAID:	Fitting Tool for Arrays of Interrelated Datasets
FT:	Fourier transformation	GABA:	γ-aminobutyric acid
Gln:	glutamine	Glu:	glutamate
GSH:	glutathione	GW:	Gaussian width
HES:	half echo sampling	MES:	maximum echo sampling
MRS:	magnetic resonance spectroscopy	NAA:	N-acetylaspartate
PRESS:	Point RESolved Spectroscopy	TE:	echo time
TR:	repetition time		

An alternative route to arrive at optimal parameters for a particular experimental setting is to calculate the expected lower bound of the achievable precision for a range of potential experimental situations and select the experiment with best precision for the targeted metabolites. The so-called Cramér-Rao minimum variance bounds (CRBs) (Cavassila et al., 2001) are an ideal measure for such an approach. CRBs provide a lower bound for the variance of fitted parameters and thus can be used as a measure for the maximum precision attainable by a specific experiment if the model for the data is complete and correct. In addition, they can be estimated without actually acquiring spectra, but purely based on a parameterized model function and the expected signal-to-noise ratio (SNR). This method of experiment optimization has been used in different fields (Anastasiou and Hall, 2004; Brihuega-Moreno et al., 2003; Ober et al., 2002) but only preliminary results of its use for in vivo MRS have been reported (Bolliger et al., 2012; Chong et al., 2007; Snyder and Lange, 2012).

To demonstrate the principle, we investigated the optimization of localized one- and two-dimensional spin echo experiments of human brain. The one-dimensional case corresponds to the clinically most frequently used localization sequence, PRESS (Point RESolved Spectroscopy (Bottomley, 1984)), with the echo time as an optimizable parameter and with a linear combination model of basis sets as evaluation tool. Simultaneous evaluation of multiple spectra with differing echo times corresponds to 2D J-separation spectroscopy (2DJ MRS or J-PRESS) (Aue et al., 1976; Kreis and Boesch, 1994; Thomas et al., 1996; Thomas et al., 2003), where a series of PRESS scans is acquired with TE incremented by a fixed step size, thus obtaining a two-dimensional dataset, which is usually Fourier transformed in both dimensions before evaluation. 2DJ-MRS has been recommended (Roussel et al., 2010; Schulte et al., 2006) for simultaneous quantification of brain metabolites, and it has been claimed previously (Gonenc et al., 2010) that in particular the quantification of coupled metabolites is improved with 2DJ compared to 1D experiments. The benefit of acquiring multiple echo data in single shots and Monte Carlo parameter optimization in view of a compromise between spectral resolution and added information from multiple echoes was described in Ref. (Kiefer et al., 1998).

Here, 2DJ experiments are considered where no Fourier transformation (FT) is applied in the second dimension and which can be evaluated with a linear combination model with prior knowledge relations like in the 1D case using FiTAID (Fitting Tool for Arrays of Interrelated Datasets) (Chong et al., 2011). This provides the freedom to combine scans of arbitrary echo

times (i.e. not equally-spaced timings) and arbitrary number of scans per TE. This so-called *generalized 2DJ experiment* was thus optimized with CRBs criteria for optimal precision for a targeted set of metabolites.

Acquiring a series of PRESS scans with varying TEs has two main advantages over single short TE experiments: First, it allows for the fitting of transverse relaxation times and second, J-coupled spins undergo J-evolution, which leads to specific spectral patterns as function of TE (or cross-peaks in 2D spectra after double FT) and therefore better discrimination between metabolites. Short TE scans have the advantage of a higher signal-to-noise ratio, but this comes at the expense of large underlying macromolecular signals. Due to their short transverse relaxation time compared to metabolites, it is possible to eliminate macromolecular signals by using long enough TE while maintaining metabolite signals – though they are evidently reduced by relaxation and phase dispersion through J-evolution, as well. Therefore, sampling short as well as long echo times in one experiment may possibly improve the discrimination of macromolecules and metabolites.

Here, we propose the principle of using CRBs for MRS experiment design and illustrate it by determining whether short TE spectra, conventional, or generalized 2DJ scans are the best for the quantitation of specific brain metabolites. Additionally, the question was addressed which TE to use in 1D MRS and which maximum TE and TE spacing are best suited in conventional 2DJ scans for the quantitation of the metabolites of interest. Exemplary interest was placed on γ-aminobutyric acid (GABA), glutamate (Glu), glutamine (Gln) and glutathione (GSH). Model simulations were used to identify general characteristics, while in vivo spectra were recorded to demonstrate the general validity of this design approach. In order to document small improvements in quantification precision in vivo, a large number of repeated measurements in human subjects is needed. However, the scan time that can be tolerated by individual subjects is limited. Therefore the number of repeated measurements was extended artificially by bootstrapping (Efron, 1979), which has turned out to be a very useful technique to estimate probability distributions and has previously been used in in vivo MRS in order to estimate errors of fitting parameters (Bolan et al., 2004) based on resampled subsets of individually stored single MRS acquisitions.

2. Material and Methods

2.1. Estimation of CRBs

CRBs provide a lower bound of the standard deviation ρ_{pl} for the parameters p_l of a model function ξ fitted to experimental data by minimizing χ^2, provided that the parameter estimator is unbiased and the SNR is above a certain threshold (Vallisneri, 2008). For the estimator to be unbiased and thus for the CRBs to yield valid bounds for the physical variables described by the fitting parameters, the model has to be correct and the minimization procedure has to provide the global minimum. Besides, the model has to be fully parameterized. The CRBs are obtained using the Fisher information matrix F, by extracting the roots of the corresponding diagonal elements of its inverse:

$$\rho_{p_l} \geq CRB_{p_l} = \sqrt{(F^{-1})_{ll}} \qquad \textit{[Eq. 1]}$$

As described in Ref.(Cavassila et al., 2001), F can be calculated by taking the real part of a complex-valued matrix product:

$$F = \Re(D^H D)\,, \qquad \textit{[Eq.2]}$$

where H denotes Hermitian conjugation. The columns of the matrix D are partial derivatives of the discretized model function ξ_n (where n denotes the data point index of the measured data, possibly a multi-dimensional index) with respect to the fitted parameters

$$D_{nj} = \frac{1}{\sigma_n} \cdot \frac{\partial \xi_n}{\partial p_j}, \qquad \textit{[Eq. 3]}$$

where σ_n is the standard deviation of the noise at the respective data point. Here, we assume equal standard deviations at all data points, i.e. σ_n=σ, thus the CRBs depend linearly on σ.

In order to obtain the matrix [2] D, the partial derivatives should be evaluated at the true parameter values. In practice, however, these values are unknown and D is estimated with fitted parameter values.

In addition, the information matrix is invariant under FT of the data since the FT preserves the inner product. Therefore, CRBs can be calculated in either time or frequency domain. This applies to both, the directly measured dimension and the indirect (second) dimension.

In the context of trying to understand which particular subsets of 2DJ data are most relevant for generalized 2DJ experiments, it is worthwhile to note that the inverse of the diagonal elements of the Fisher matrix provide a lower bound to the respective CRB, since for any positive definite matrix it can be shown that $(F_{kk})^{-1} \leq (F^{-1})_{kk}$. (The proof is presented in the inline supplement P.1.)

Furthermore, in the case of a complete model, decreasing the number of data points by selecting a limited data range in any dimension cannot decrease the CRBs. (inline supplement P.2 contains the proof for the equivalent statement that extending the data range from a selected region leads to decreased or at least invariant CRBs).

2.2. Specific model function

While the principle of using CRBs criteria to optimize experimental parameters is valid for arbitrary experiments and independent of the formulation of the signal model (as long as it is

[2] Typically, in a valid model, the rows of D are linearly independent and hence the corresponding Fisher information matrix is positive definite and the inverse exists. However, under certain circumstances it is possible that the Fisher matrix becomes singular (or nearly singular, i.e. ill-conditioned), in which case F^{-1} in equation [1] can be replaced by the Moore-Penrose pseudoinverse $F^{\dagger}$ of F (Vallisneri, 2008). This is usually a sign that prior knowledge should be applied to the parameters that cause the singularity.

complete and correct), a localized 2DJ experiment and the model function as previously defined in Ref. (Chong et al., 2011) was used to illustrate the claim. In short, the model describes a two-dimensional parameterized function consisting of a linear composition of simulated two-dimensional basis sets $\xi_k^{Num}(t_{n1}, TE_{n2})$ where k is an index usually referring to the different two dimensional basis spectra of the included metabolites and the superscript Num symbolizes the fact that the basis spectra refer to numeric patterns. Often the basis sets are linked by prior knowledge constraints in both dimensions. For half echo sampling (HES), they can be explicitly summarized as:

$$\xi_{n1,n2}^{HES} = \xi^{HES}(t_{n1}, TE_{n2}) = \sum_k A_k \exp(\mathrm{i}\varphi_k) \exp\left(-\frac{\pi^2 GW_k^2}{4\ln 2} t_{n1}{}^2\right) \cdot \exp\left(-(t_{n1} + TE_{n2})/T_2^{(k)}\right) \xi_k^{Num}(t_{n1}, TE_{n2}),$$

[Eq. 4]

where the area (A_k)[3], phase (φ_k), transversal relaxation time ($T_2^{(k)}$), and the Gaussian width (GW_k) are fitting parameters for the individual basis functions. Introducing prior knowledge reduces the number of free parameters. In the specific models used below, the Gaussian widths were identical for all metabolites (representing field inhomogeneities affecting all metabolites equally), and the T_2s of all coupled spins were linked to a common T_2 parameter, resulting in only 5 different T_2s in the model.

For data acquired with maximum echo sampling (MES) (Kiefer et al., 1998; Macura and Brown, 1983; Schulte et al., 2006), the model has to be adjusted. More precisely, for a time domain signal for which data sampling was started t^{ED} before the echo maximum, the model is adjusted as follows:

[3] We refer to A, the time domain signal amplitude, as (frequency domain) area parameter, rather than amplitude, while the word amplitude is used for the frequency domain peak amplitude.

$$\xi_{n1,n2}^{MES} = \xi^{MES}(t_{n1}, TE_{n2}, t_{n2}^{ED})$$
$$= \sum_k A_k \exp(\mathrm{i}\varphi_k)\ \exp\left(-\frac{\pi^2 GW_k^2}{4\ln 2}(t_{n1} - t_{n2}^{ED})^2\right) \exp\left(-\frac{(t_{n1} + TE_{n2} - t_{n2}^{ED})}{T_2^{(k)}}\right) \xi_k^{Num}(t_{n1}, TE_{n2}, t_{n2}^{ED}).$$

[Eq. 5]

Note that HES corresponds to MES with an echo delay t^{ED} of 0 ms:

$$\xi_{MES}(t, TE, t^{ED} = 0) = \xi_{HES}(t, TE).$$ [Eq. 6]

Basis spectra $\xi_k^{Num}(t_{n1}, TE_{n2}, t_{n2}^{ED})$ for 18 metabolites were simulated for 3T in GAVA (Soher et al., 2007), using chemical shifts and J-couplings from Refs. (Govindaraju et al., 2000) and (Tchong Len et al., 2004). Of major importance in the current context is the modeling of the macromolecular baseline (MMBL). In order for the concept of CRBs use for experiment optimization to be valid, the MMBL must be included in a parameterized form (or reliably and accurately be eliminated in preprocessing) (Cudalbu et al., 2012). As in Ref. (Chong et al., 2011), an experimentally measured MMBL was included, parameterized as equally spaced Voigt lines with sets of common line widths and T_2s.

Calculation of CRBs and general data processing was performed in matlab version 7.4.0 R2007a (Mathworks, Natick, Massachusetts, U.S.A.). The data was fitted as a 2D-array without FT along the second dimension.

2.3. Optimization of experimental parameters

Optimal experiments were designed by calculation of expected CRBs for a large set of conventional and generalized 2DJ experiments based on the model function described in 2.2 and specified below. The optimizations were performed for typical in vivo conditions of human brain. In particular, the following parameter values were used:

a) linewidth parameters chosen to correspond to typical values as obtained from fitting 2DJ datasets recorded from a volume in occipital human gray matter (Gaussian line width of 4 Hz and natural linewidths ($^{1}/_{(\pi \cdot T_2)}$) for metabolites ranging from 1.0 to 2.5 Hz)

b) area parameter values selected to correspond to typical metabolite concentrations, and

c) the MMBL described as three partially linked subparts as in Ref. (Chong et al., 2011).

For all PRESS experiments considered here, the time interval between the 90° pulse and the first 180° pulse was kept fixed at 6 ms, and for MES the signal acquisition started 5 ms after the second 180° pulse, such that $t^{ED} = TE/2 - 11\text{ms}$. Thus, for these settings HES coincides with MES at TE=22 ms.

2.3.1. 1D MRS and conventional 2DJ scans

In order to determine the longest echo time to be included and to find optimal TE spacings, CRBs were estimated for all possible 1D and 2DJ experiments with a lower limit for TE of 22 ms, TE step sizes of 0 or multiples of 2 ms, and an upper limit for TE of 322 ms. HES, as well as MES, was considered. For a meaningful comparison, experiments with equal acquisition time have to be evaluated, thus, the standard deviation of the noise for the estimation of the CRBs was scaled by $\sqrt{N}$, where N is the number of TE steps.

2.3.2. Generalized 2DJ scans

Based on the longest TE found to be relevant in paragraph 2.3.1, minimal CRBs were searched in a set of generalized 2DJ experiments. This search covered all generalized 2DJ experiments with 8 scans and TEs in an interval between 22 ms and 202 ms, with values included with a step size of 12 ms, also allowing multiple scans with identical TE.

Experiments yielding minimal CRBs for GABA, Glu, Gln and GSH were identified as well as an experiment dedicated to GABA and Glu quantification, where the experiment with minimal CRB for Glu was selected from all experiments with GABA CRBs that were at most 1% larger than the GABA optimum.

2.4. Factors influencing optima in experiment design

Optima of generalized experiments were obtained for a number of different situations to evaluate dependences between these factors and the CRB optima. The following five factors were investigated by searching for optima in specific experiment or model situations:

1. MES: half vs. maximum echo sampling.
2. Shim: varying the Gaussian linewidth from 2, to 4, 6, and 8 Hz.
3. T_2 estimation: inclusion vs. exclusion of T_2s as fitting variables.
4. MMBL estimation: inclusion vs. exclusion of the MMBL as fitting parameters.
5. Model complexity: hypothetical simple situation of only 5 metabolites without MMBL vs. the full model. In this case, only the areas of the 5 metabolites were fitting parameters.

2.5. Verification on simulated data

The improvement in quantification precision predicted by the respective CRBs was verified in a first step on simulated data. For an optimized and a conventional 2DJ experiment, a set of 130 spectra each was constructed by adding different noise realizations to the model data.

The optimized experiment considered was the generalized 2DJ found to be optimal for Glu quantitation (for which the acquisition of the signal for TE=22 ms was repeated 6 times and the echo times of 58 ms and 202 ms were acquired once each), and the echo times considered for the conventional 2DJ experiment were 22 ms up to 246 ms, incremented in steps of 32 ms. In both cases, MES was assumed. The noise added to the data was realized as white Gaussian noise, such that an SNR of 45.6 (defined by the maximum peak amplitude (methyl singlet of NAA) at TE=22 ms) was obtained.

A power analysis for the F-test was used to calculate the sample size needed to prove that the variance in the results for Glu is smaller from the generalized 2DJ experiment than from the conventional 2DJ. For the expected difference in standard deviations (20% decrease), a significance level α of 0.05, and a power of 0.8, the minimum sample size came out to be 126 for each 2DJ variant (Lenth, 2012).

The parameters for each simulated experiment were fitted in FiTAID, where basis spectra simulated for 18 metabolites with Voigt lineshapes were applied and where the Lorentzian widths were coupled with the respective T_2s. Only 5 different metabolite T_2s were introduced: a common T_2 for all multiplets, and individual T_2s for the singlets of Cr, NAA, and total choline.

Standard deviations for the fitted Glu concentrations were calculated. In order to exclude effects of those cases where the fitting procedure terminated in a local χ^2 minimum, outliers were excluded by removing values that lay outside the mean ±2 standard deviations of the whole set and were outside of the range defined by the mean ± 3 standard deviations of the reduced set.

The one-sided F-Test was used to compare the variances of the Glu area parameters obtained from the selected conventional and generalized 2DJ scans

2.6. In vivo verification

In order to verify the predicted precision improvement in vivo, human brain spectra were recorded in 8 healthy subjects (6 female, 2 male, age 35.0±12.9 years) from a region of interest of 15.4 cm^3 in occipital grey matter on a 3T Siemens Trio scanner using a quadrature transmit/receive head coil. The standard 2DJ experiment (8 TEs from 22 to 246 ms, in steps of 32 ms, 16 acquisitions per TE), as well as an optimized generalized experiment (TEs of 22ms, 22ms, 58ms, 22ms, 22ms, 202ms, 22ms, and 22ms, 16 acquisitions per TE), was recorded for each subject 6 times in an interleaved fashion (5.5 min acquisition time each, TR 2.5 s) in a single session. MES was used, as described in chapter 2.3. Metabolite cycling (MacMillan et al., 2011) was applied instead of water presaturation in order to obtain the metabolite and reference spectra simultaneously. Post processing included adding/subtracting the metabolite-cycled scans to obtain metabolite and water spectra (used for eddy current correction) and Hankel-Lanczos Singular Value Decomposition (Pijnappel et al., 1992) to eliminate the residual water signal.

Bootstrapping was used to create 25 out of the recorded 6 datasets for both the standard and the optimized experiment in each subject. Each data point of the bootstrapped spectra was obtained by random sampling from the corresponding 6 complex-valued data points of the (frequency-aligned and post-processed) original spectra. Each spectrum was fitted independently with FiTAID as described above in chapter 2.5, except for an additional overall shift parameter. The bootstrap estimate of the standard deviations of the fitted parameters, i.e. the variance of the bootstrapped dataset, was used as an approximation of the true standard deviation, which yields a more precise approximation than the variance of the original data based on 6 values only. Outlier removal was performed as described earlier, and a general linear model was applied for the fitted parameter of interest to determine the experimental variance ε controlling for inter-individual differences in metabolite content.

3. Results

3.1. Optimization of experimental parameters

3.1.1. 1D PRESS and conventional 2DJ MRS

CRBs optimization of experimental conditions is first illustrated for standard single TE spectra. Exemplary results for the optimization of 1D PRESS experiments are shown in Figure 1. The CRBs are plotted for 3 metabolites as a function of TE (full lines). Both traditional half echo sampling (Fig 1a) and MES (Fig 1b) were investigated. In both cases, there is no monotonic increase of CRBs with TE in spite of the decreasing signal due to T_2 relaxation. With HES, short TEs are advantageous for all presented metabolites. In particular, the shortest TE clearly yields the lowest CRB for Glu, while for NAA, where the spectrum is dominated by the monotonously decreasing singlet signal, the CRB increase is weaker with increasing TE. For GABA, however, the CRBs decrease somewhat with echo times from 22 ms to around 110 ms.

When MES is applied, the CRBs are lowest at different TE values for each metabolite, clearly suggesting different optimal acquisition conditions for each metabolite. In particular, for the specific fitting conditions (i.e. prior knowledge, known MMBL form, and fixed T_2s) the use of the shortest available TE is only optimal for the determination of Glu, while for GABA the use of fairly long TEs yields lower CRBs. Minima are reached for TEs around 100 and 190 ms. In the case of NAA, shorter echo times are beneficial, not only for HES, but also MES.

The CRBs are bounded from below by the inverse square root of the integrated power of the partial derivative function (for area parameters, the latter corresponds to the basis function itself). To motivate some of the TE dependence of the CRBs, this lower bound is included in Figure 1 as dashed line. The difference between these values and the CRBs is due to the correlations between fitted parameters.

For conventional 2DJ experiments, it was first evaluated up to which maximum TE data sampling should be extended and second what echo spacing would prove to be most efficient. In Figure 2, the estimated CRBs of conventional 2DJ experiments are plotted versus the maximum sampled TE in the case of dense sampling (2 ms step size). For GABA, the CRBs reach minima at 128 ms (HES) and at 208 ms (MES). With HES, the single short TE experiment is best for Glu, but for MES the minimum CRB is reached at 94 ms, with hardly any substantial

further change for maximum TEs up to around 200 ms. Above this value, the CRBs increase steadily. Interestingly, an almost monotonic exponential decrease of CRBs is observed for NAA in the cases of HES as well as MES. Up to maximum TEs of ~100 ms, the decrease in CRBs is fast.

In the bottom row of Figure 2, the ratio in CRBs for MES versus HES is illustrated as a function of maximum TE. MES is beneficial for all metabolites and all TEs. The decrease in CRBs for maximum TEs above 200 ms is as much as 25%.

The influence of step size and maximum TE on CRBs for conventional 2DJ experiments (with MES) can be appreciated from Figure 3. In the upper row, the CRBs for three metabolite areas and a linewidth are plotted versus the maximum TE for different step sizes. Below, the CRBs of a subset of these experiments are drawn as a function of step size. It seems that fine sampling is beneficial for GABA, whereas for the other parameters coarser sampling yields lower CRBs. For Lorentzian widths, and hence, T_2s, CRBs decrease monotonically with increasing maximum TE, though only with little further improvements above 200 ms.

Apparently, including maximum TEs larger than 200 ms is not efficient, not even when taking into account larger step sizes. Hence, a maximum TE of 202 ms was chosen for the optimization of generalized 2DJ experiments with MES.

Some quantitative results for the optimization of conventional 2DJ scans are assembled in the upper part of Table 1 for the strongly coupled metabolites GABA, Glu, Gln, and GSH. CRB based parameter optimization found the largest potential for improvement for Glu, with a 16% CRB decrease relative to the reference experiment. For GABA, this improvement was only a few percent. As illustrated in Figure 4, optimal conventional 2DJ experiments for Glu, Gln and GSH consist of only two or three echo times with coarse TE sampling. As already evident from Figure 3, the quantitation of GABA benefits from finer TE sampling.

3.1.2. Generalized 2DJ MRS

The expected precision improvements for generalized vs. conventional PRESS and 2DJ experiments are illustrated in the bottom part of Table 1 and Figure 4. Only small further improvements can be achieved by generalizing the TE spacings and the distribution of acquisition time per TE. The quantitation of Glu and GABA benefit most from generalization with decreases in CRBs of 5 % and 4 %, respectively, while for Gln and GSH hardly any

improvement can be achieved. For the quantitation of Glu and Gln, experiments consisting of a combination of several repetitions of the shortest TE and shorter measurements of longer TEs are favorable, whereas for GABA and GSH the emphasis is on longer TE (see Fig. 4). Table 1 illustrates also that optimizing experimental conditions for one metabolite often worsens the precision for others. If several metabolites are of interest, other experiments that compromise for the set of metabolites can be chosen. If one is, for example, mostly interested in the neurotransmitters GABA and Glu, one might opt for the experiment listed in the last row, which was found as the best setup for Glu among those scans that are within 1% of the optimum achievable for GABA. This compromise yields almost the maximum improvement for GABA with hardly any penalty for Glu (or the other listed metabolites).

3.2. Effects of model/experiment on optima

The extent of the CRBs improvement and the optimal experimental parameters found for any specific metabolite depend on the exact experimental or model situation considered. To demonstrate this, generalized 2DJ experiments optimized for the quantification of 3 different metabolites are depicted in Figure 5 for various scenarios. The figure also shows percentage CRBs improvements for each case in relation to its own corresponding conventional 2DJ experiment with TEs from 22 ms to 246 ms.

HES was compared to MES, both for the full model and for a simplified case of only 5 metabolites (see Methods, all with GW of 4Hz). In both cases, it was found that optimized experiments tend to include shorter TEs in the case of HES. In addition, the potential for CRBs improvements is clearly larger for HES than MES, which is mostly due to the fact that there is larger SNR loss for HES than MES with increasing TE.

The influence of line broadening (shim performance) on the optimal scans can be seen from the comparison of the evaluations for models with different Gaussian widths. For broader lines, the shortest TE scans are weighed less, probably because of the larger correlation between metabolites and the MMBL. In agreement with this, the shortest TE tends to have more weight if the MMBL is not fitted (assumed to be known or removed in a preprocessing step).

If T_2 relaxation times are not fitted but kept fixed (possibly taken from a cohort average) the scans with the longest TEs lose importance and are replaced with shorter TE scans that have less T_2-weighting.

If the model complexity is reduced to the inclusion of only 5 metabolite areas, the optimal experiments change noticeably, but there does not seem to be a clear trend on how they change.

In addition, there are some metabolite-specific observations. For GABA, in the case of MES, the single TE PRESS experiment with TE=166 ms is superior to all generalized 2DJ experiments in the case where only the area parameters of five metabolites are fitted. This TE is also distinctively present in the optimized experiments when more parameters are fitted or when the Gaussian line width is varied. For HES, the most relevant TE seems to be 94 ms. However, the overall potential for improvement seems to be rather small for GABA.

For Glu, in all cases a combination of repeated measurements at the shortest TE combined with fewer scans at longer TE is optimal. These experiments decrease the CRBs by 20% and more for most cases. The optimal experiments for the quantitation of NAA show similar patterns, though with a slightly lower potential for improvement.

3.3. Verification on simulated data

Monte Carlo fits of an in silico dataset, where the ground truth is known, were used to test whether the improvement in estimation precision, as predicted by the CRBs criterion used in experiment design, does indeed hold. The CRB for Glu quantification was expected to be 7.9% and 5.6% for the conventional and the optimized experiments. Least squares optimizations in 130 experiments each yielded coefficients of variance for the two cases of 5.6% and 4.0% and showed that there was no significant bias of the estimated concentrations in either experiment. The one-sided F-test showed that the variance of the fitted Glu concentrations for the optimized experiment is significantly lower than for the conventional 2DJ experiment ($p=0.0005$).

3.4. In vivo verification

The same experiments were tested also on in vivo data acquired in 6 measurements in 8 subjects. In Figure 6, sample spectra obtained for the conventional and the generalized 2DJ experiment optimized for Glu are presented (6 spectra with TE=22 ms plotted as an average with improved SNR). The six repeats per subject were extended to 25 pseudo-repeats by bootstrapping (see Methods for details and the inline electronic supplement for a figure to illustrate this procedure). The results for Glu from 2D model fitting of the conventional and the

generalized 2DJ experiments in 8 subjects are presented in Figure 7. The quantitative analysis of the fitted Glu concentrations confirmed the prediction. The coefficient of variance decreased to 66% of the value obtained for the conventional experiment, while the CRBs calculations had forecast an improvement of the variance to 80%.

4. Discussion

CRBs provide well-suited criteria to select optimal sampling strategies for many applications and fields. Here, it was shown that the CRBs criteria can be very beneficial for the optimization of acquisition parameters of localization and quantification sequences used in clinical MRS and in combination with linear combination model fitting. In particular, this was illustrated for the optimization of 2D experiments targeted at specific individual or groups of metabolites of interest in neuroresearch.

The proposed principle is valid for any MRS technique where the results are obtained by unbiased least squares fitting with a complete model. As shown in the examples, specific potential for CRBs as design criteria is not only found for complex experiments like the generalized 2DJ, but even for the most standard 1D localization sequence in clinical use. However, the basic principle was illustrated primarily for the more complex situation of the 2D J separation experiment that is becoming more and more popular in brain research at clinical field strengths for a simultaneous and more accurate determination of coupled metabolites. Conventional or generalized 2DJ experiments, i.e. acquisitions of a series of PRESS scans with varying TEs, have several advantages over single short TE experiments: First, they provide for determination of transverse relaxation times. Second, because J-coupled spins show specifically varying spectral patterns as function of TE (or cross-peaks in doubly Fourier-transformed 2D spectra), 2DJ has the potential for better discrimination between metabolites. And third, 2DJ experiments benefit from maximum-echo sampling where signal acquisition starts immediately after the last RF pulse rather than at the echo maximum (Kiefer et al., 1998; Macura and Brown, 1983; Schulte et al., 2006). Here, it was demonstrated how acquisition parameters for conventional and generalized 2DJ experiments can be optimized in order to manifest the purported advantages. Expected CRBs were estimated for a set of experiments and those with minimal CRB for a parameter of interest were considered optimal. Optima depend on which metabolites are prioritized, but also on experimental circumstances, like shim

quality, or on whether or not the MMBL or metabolite T_2s are expected to change or are assumed to be constant.

In terms of specific optimization results, it is most noteworthy that it has been shown quantitatively that MES provides a large benefit for all metabolites and that careful selection of the maximum TE and the TE spacing in conventional 2DJ can substantially lower the CRBs further. For the typical in vivo T_2 values, the maximum useful TE amounted to about 200 ms in the case of MES and fairly large TE spacing seemed optimal for most metabolites. Generalization of the 2DJ sampling strategy did not lead to dramatic further improvements.

Interestingly, optimal experiments for Glu and NAA contain at least one scan with the shortest TE of 22 ms, but this is not the case for GABA, which is in agreement with the optimized single TE experiments and a recent study (Napolitano et al., 2013). It is certainly of note that optimal 1D experiments for some metabolites may ask for longer echo times and that also for the 1D experiments one may well benefit from MES, a strategy that is currently hardly ever pursued.

It should be stressed that the estimated CRBs are strictly only valid for the specific circumstances considered (e.g. field strength, ideal RF pulses, line width, metabolite set) and the case of a complete model where the treatment of the baseline is crucial. This certainly limits this approach for experiment design, however, being able to finetune the acquisition strategy to the exact experimental situation (e.g. field strength), or postprocessing strategy, is also an advantage. For example, it makes sense to use different experiments whether or not the T_2s or MMBL will be treated as unknown.

The inverse of the square root of the diagonal elements of the Fisher matrix do not depend on the prior knowledge applied to the other parameters and provide a lower bound to the respective CRBs. They might thus be used as an approximation. However, conclusions from this approximation can be misleading, as seen in the case of GABA.

Alternative methods for parameter optimizations mostly aiming at specific metabolites have often been based on finding the best acquisition parameters for optimal target signal yield but also with minimal spectral overlap between the target and nuisance signals (Choi et al., 2010; Choi et al., 2012; Hu et al., 2007; Kim et al., 2005; Snyder and Wilman, 2010), usually based on quantum mechanical simulations and in vitro experiments. These investigations certainly have the advantage of yielding basic understanding of why certain parameter settings are optimal, but the CRBs inherently provide a tool that includes these optimization criteria and also extends them to other interfering metabolites and experimental factors.

One considerable advantage of the proposed strategy is the possibility to optimize experiments not just for single but also for multiple metabolites. If the optimum for two parameters is targeted, an approach as presented for the quantification of GABA and Glu can be chosen, where the experiment yielding minimal CRB for Glu has been selected from all experiments yielding close to the minimal CRB for GABA. As an alternative, or if the optimum for a larger set of parameters is required, criteria used in multi-objective optimization, such as Pareto-optimality (Bolliger et al., 2011) or weighted sums, can be applied to choose the optimal experiment.

It should be noted that CRBs, if calculated with the full data range in both domains, do not depend on whether FT is applied in the 2nd dimension or not. Furthermore, in the case of a complete model, neglecting any information leads to an increase in CRBs. Therefore, restriction of χ^2 calculation to off-diagonal areas (in the 2D FT case) does not help - on the contrary. This might be different if the model is incomplete (e.g. unknown baseline that cannot properly be parameterized) and off-diagonal regions in the 2D spectrum might be virtually unaffected by the unknown baseline components that interfere in the overall model.

The verification of the proposed strategy of experiment optimization was performed in two steps for a specific 2DJ experiment optimized for quantification of Glu: First, using synthetic spectra where the true parameter values are known, and second for in vivo spectra. In the latter case, where the number of experiments that can be acquired per volunteer is limited, bootstrapping was used to artificially increase the number of experiments acquired for every volunteer for a better estimation of the variance of the fitted parameters. However, this approach cannot be used to artificially expand on the number of volunteers because inter-individual differences interfere with bootstrapping. It should be noted that in absolute terms the standard deviations obtained with bootstrapping are slightly lower than the true values because of induced correlations. However, for performance comparison of the two experimental settings, standard deviations from bootstrapped data are perfectly valid.

Both verification approaches confirmed the improvement of quantitation precision that had been predicted by the CRBs estimations, which were based solely on a theoretical model. Using the synthetic model, where the true parameter values were known (and corresponded exactly to the values used for the CRBs estimation), it was shown that the accuracy of the fitted parameters was not degraded by using the optimized experiment. The improvement in quantitation precision in the in vivo case was in surprisingly good agreement with the prediction, in spite of the differences between the parameter values used for CRBs estimation and the fitted parameters,

and in spite of the limitations in the model, like the description of the macromolecular baseline as a set of mono-exponentially decaying Voigt lines, which is not true as known from GABA editing (Henry et al., 2001).

5. Conclusions

Localized MR spectroscopy experiments can be optimized for best use of scan time for particular target metabolites using Cramér-Rao bounds criteria. Specifically, for conventional 2DJ experiments, best maximum TE to be included and best echo spacing can objectively be defined. Furthermore, CRBs criteria can be used to generalize the 2DJ experiment to allow unequal echo spacing and unequal number of acquisitions per TE. The benefit of maximum echo sampling has been documented quantitatively, not only for 2DJ, but also common 1D PRESS. The principle of experiment design based on CRBs optimization has been illustrated and verified with artificial spectra, but also in vivo brain spectra where the parameter optimization was documented with the expected improvement of variance in fitting results for Glu. It was also shown that bootstrapping can be used to effectively extend the measurement time beyond what is normally tolerable by human subjects. The CRBs method has clear limits that have to be respected, including the need for a correct model and full model parameterization.

6. Tables

Table 1:

Relative Cramér- Rao minimum variance bounds for selected experiments as presented in Fig. 4 and scaled for equal scan time. CRB values for all included area parameters are listed as relative values with respect to the corresponding CRBs in the default conventional 2DJ experiment provided in the top trace.. Further rows contain conventional 2DJ experiments optimized for the metabolite listed in the first column; the darker shaded area contains generalized 2DJ experiments optimized for either individual metabolites, or in the lowest row for GABA and Glu (cf. text). All scans include MES and T_2 fitting.

7. Figure captions

Figure 1:

Cramér- Rao minimum variance bounds for 1D single TE scans. CRBs for single TE PRESS experiments are plotted as function of TE (solid lines) for three representative metabolite area parameters. The inverse square roots of the diagonal elements of the Fisher matrix (dashed line) provide a lower bound to the respective CRBs. The CRBs are expressed relative to the CRB value obtained for TE 22 ms. The upper row corresponds to half echo sampling and the lower row to maximum echo sampling. (Lorentzian widths not fitted, note the different scales for HES and MES).

Figure 2:

Cramér- Rao minimum variance bounds for conventional 2DJ experiments as function of maximum TE. The graphs show the influence of the maximum TE for each experiment on the CRBs for the area parameters of the same metabolites as in Fig. 1 for dense TE sampling (step size of 2 ms) but assuming equal total experiment duration (relative scaling for CRBs as in Fig. 1). The difference of MES (blue) vs. HES (red) is already evident in the top row and is further illustrated quantitatively in the lower row.

Figure 3:

Cramér- Rao minimum variance bounds for conventional 2DJ experiments as function of maximum TE and TE sampling density. Row a) shows relative CRB values of all sampled 2DJ experiments as a function of the maximal TE, while row b) zooms into the subset of experiments with maximum TE between 180 and 220 ms (blue rectangle in the upper row) and shows these selected CRBs as a function of TE step size (relative scaling for CRBs as in Fig. 1). CRBs for three metabolite areas and one linewidth parameter are shown. The data are color-coded depending on the number of steps: darker colored dots refer to finely-sampled 2DJ, brighter dots to a coarser sampling. Example: experiment consisting of TEs 22, 36, 50 ms → max TE = 50ms, TE step = 14 ms, number of steps = 3. An extended version of this figure can be found in the electronic supplement (ES1).

Figure 4:

Experimental schemes for the optimized experiments listed in Table 1. Each row represents a 2DJ experiment consisting of different TE scans as described in Table 1. The TE values used are given by number (in ms) and the width of each field represents the scan time dedicated to a specific TE.

Figure 5:

Pictorial representation of generalized 2DJ experiments optimized for GABA, Glu and NAA under different model situations. 2DJ experiments are depicted as histograms of the rate of use for each TE, hence the height of the bars represents how often the respective TE was sampled (maximum height corresponds to 8 repetitions, e.g., the top left graph represents a 2DJ experiment with 6 scans at TE 22, one scan at TE 94, and one scan at TE 118 ms). The different rows correspond to different model or acquisition conditions as stated on the left and representing:

- GW 2 Hz to 8 Hz: models with increasing overall Gaussian width (decreasing shim quality).
- no T_2: model with fixed T_2s (not fitted).

- no MMBL: model with fixed MMBL contribution, no MMBL related parameters fitted.
- 5 met: strongly simplified model with only 5 metabolites and 5 free parameters (area parameters of Cr, GABA, Glu, Gln and NAA).

Blue and red graphs represent MES and HES, respectively. The values on top of the bar plots stand for the percentage CRB decrease achieved for this case in comparison to the conventional 2DJ experiment with TEs from 22 ms to 246 ms, in steps of 32 ms (with the same model settings and acquisition scheme (HES or MES)).

Figure 6:

Representative conventional and generalized 2DJ spectra recorded from human grey matter in a healthy subject. The spectra obtained with MES and plotted in magnitude mode correspond to a conventional (A, TE 22 to 246 ms, 16 acquisitions per TE) and a generalized 2DJ experiment optimized for Glu (B, see 3rd row in Fig. 5). The higher scan time spent on TE 22 ms is evident from the lower noise in that spectrum.

.

Figure 7:

Glutamate content as obtained from 2D fitting of conventional and optimized generalized 2DJ spectra for volunteers A to H. The bars represent average values ± 1 standard deviation for the fitted Glu concentration. Left: conventional 2DJ experiment, right: optimized experiment (cf. Fig. 6). Evaluations with (orange) and without bootstrapping (black) are given.

Acknowledgements

Supported by the Swiss National Science Foundation (320030_135743). The funding source did not have any involvement in the study other than for financial support of one of the authors.

8. References

Allen, P.S., Thompson, R.B., Wilman, A.H., 1997. Metabolite-specific NMR spectroscopy in vivo. NMR in Biomedicine 10, 435-444.

Anastasiou, A., Hall, L.D., 2004. Optimisation of T2 and M0 measurements of bi-exponential systems. Magn Reson Imaging 22, 67-80.

Aue, W.P., Karhan, J., Ernst, R.R., 1976. Homonuclear broad band decoupling and two-dimensional J-resolved NMR spectroscopy. Journal of Chemical Physics 64, 4226-4227.

Bolan, P.J.A.W., Henry, P.G., Garwood, M., 2004. Feasibility of computer-intensive methods for estimating the variance of spectral fitting parameters. International Society of Magnetic Resonance in Medicine, Kyoto, p. 304.

Bolliger, C.S., Boesch, C., Kreis, R., 2011. Generalizing the 2DJ experiment for optimal simultaneous detection of a set of metabolites. 28th Annual Meeting of the European Society for Magnetic Resonance in Medicine and Biology. European Society for Magnetic Resonance in Medicine and Biology, Leipzig, Germany, p. 243.

Bolliger, C.S., Boesch, C., Kreis, R., 2012. Optimizing 2DJ experiments using Cramer Rao minimum variance bounds. 20th Annual Meeting of the International Society of Magnetic Resonance in Medicine. International Society of Magnetic Resonance in Medicine, Melbourne, Australia, p. 1752.

Bottomley, P.A., 1984. Selective volume method for performing localized NMR spectroscopy. In: General Electric Company (Ed.), U.S.

Brihuega-Moreno, O., Heese, F.P., Hall, L.D., 2003. Optimization of diffusion measurements using Cramer-Rao lower bound theory and its application to articular cartilage. Magnetic Resonance in Medicine 50, 1069-1076.

Cavassila, S., Deval, S., Huegen, C., van Ormondt, D., Graveron-Demilly, D., 2001. Cramer-Rao bounds: an evaluation tool for quantitation. NMR in Biomedicine 14, 278-283.

Choi, C., Dimitrov, I.E., Douglas, D., Patel, A., Kaiser, L.G., Amezcua, C.A., Maher, E.A., 2010. Improvement of resolution for brain coupled metabolites by optimized ^{1}H MRS at 7T. NMR in Biomedicine 23, 1044-1052.

Choi, C., Ganji, S.K., DeBerardinis, R.J., Hatanpaa, K.J., Rakheja, D., Kovacs, Z., Yang, X.L., Mashimo, T., Raisanen, J.M., Marin-Valencia, I., Pascual, J.M., Madden, C.J., Mickey, B.E., Malloy, C.R., Bachoo, R.M., Maher, E.A., 2012. 2-hydroxyglutarate detection by magnetic resonance spectroscopy in IDH-mutated patients with gliomas. Nat Med 18, 624-629.

Chong, D.G.Q., Kreis, R., Bolliger, C., Boesch, C., Slotboom, J., 2011. Two-dimensional linear-combination model fitting of magnetic resonance spectra to define the macromolecule baseline using FiTAID, a Fitting Tool for Arrays of Interrelated Datasets. Magn Reson Mater Phy 24, 147-164.

Chong, D.G.Q., Slotboom, J., Kreis, R., 2007. Feasibility of using predicted Cramer Rao lower bounds for the design of optimized in vivo MR spectroscopy sequences targeting multiple metabolites. International Society of Magnetic Resonance in Medicine, Berlin, p. 1406.

Cudalbu, C., Mlynarik, V., Gruetter, R., 2012. Handling macromolecule signals in the quantification of the neurochemical profile. J Alzheimers.Dis 31 Suppl 3, S101-S115.

Efron, B., 1979. Bootstrap methods: another look at the jackknife. The annals of Statistics 7, 1-26.

Gonenc, A., Govind, V., Sheriff, S., Maudsley, A.A., 2010. Comparison of spectral fitting methods for overlapping J-coupled metabolite resonances. Magnetic Resonance in Medicine 64, 623-628.

Govindaraju, V., Young, K., Maudsley, A.A., 2000. Proton NMR chemical shifts and coupling constants for brain metabolites. NMR in Biomedicine 13, 129-153.

Henry, P.G., Dautry, C., Hantraye, P., Bloch, G., 2001. Brain GABA editing without macromolecule contamination. Magnetic Resonance in Medicine 45, 517-520.

Hu, J., Yang, S., Xuan, Y., Jiang, Q., Yang, Y., Haacke, E.M., 2007. Simultaneous detection of resolved glutamate, glutamine, and gamma-aminobutyric acid at 4 T. J Magn Reson 185, 204-213.

Kiefer, A.P., Govindaraju, V., Matson, G.B., Weiner, M.W., Maudsley, A.A., 1998. Multiple-echo proton spectroscopic imaging using time domain parametric spectral analysis. Magnetic Resonance in Medicine 39, 528-538.

Kim, H., Thompson, R.B., Hanstock, C.C., Allen, P.S., 2005. Variability of metabolite yield using STEAM or PRESS sequences in vivo at 3.0 T, illustrated with myo-inositol. Magnetic Resonance in Medicine 53, 760-769.

Kreis, R., Boesch, C., 1994. Liquid-crystal-like structures of human muscle demonstrated by *in vivo* observation of direct dipolar coupling in localized proton magnetic resonance spectroscopy. Journal Magnetic Resonance Series B 104, 189-192.

Kreis, R., Slotboom, J., Hofmann, L., Boesch, C., 2005. Integrated data acquisition and processing to determine metabolite contents, relaxation times, and macromolecule baseline in single examinations of individual subjects. Magnetic Resonance in Medicine 54, 761-768.

Lenth, R.V., 2012. Java applets for power and sample size [Computer software]. Retrieved July 2012 from http://www.stat.uiowa.edu/~rlenth/Power.

MacMillan, E.L., Chong, D.G.Q., Dreher, W., Henning, A., Boesch, C., Kreis, R., 2011. Magnetization exchange with water and T1 relaxation of the downfield resonances in human brain spectra at 3.0 T. Magnetic Resonance in Medicine 65, 1239-1246.

Macura, S., Brown, L.R., 1983. Improved sensitivity and resolution in two-dimensional homonuclear J-resolved NMR spectroscopy of macromolecules. Journal of Magnetic Resonance 53, 529-535.

Napolitano, A., Kockenberger, W., Auer, D.P., 2013. Reliable gamma aminobutyric acid measurement using optimized PRESS at 3 T. Magnetic Resonance in Medicine 69, 1528-1533.

Ober, R.J., Lin, Z., Ye, H., Ward, E.S., 2002. Achievable accuracy of parameter estimation for multidimensional NMR experiments. J Magn Reson 157, 1-16.

Pijnappel, W.W.F., van den Boogaart, A., de Beer, R., van Ormondt, D., 1992. SVD-based quantification of magnetic resonance signals. Journal of Magnetic Resonance 97, 122-134.

Provencher, S.W., 1993. Estimation of metabolite concentration from localized in vivo proton NMR spectra. Magnetic Resonance in Medicine 30, 672-679.

Ratiney, H., Sdika, M., Coenradie, Y., Cavassila, S., van Ormondt, D., Graveron-Demilly, D., 2005. Time-domain semi-parametric estimation based on a metabolite basis set. NMR in Biomedicine 18, 1-13.

Roussel, T., Cavassila, S., Ratiney, H., 2010. Sampling strategy effects on in vivo 2D J-Resolved spectroscopy quantification. International Society of Magnetic Resonance in Medicine, Stockholm, p. 904.

Schulte, R.F., Boesiger, P., 2006. ProFit: two-dimensional prior-knowledge fitting of J-resolved spectra. NMR in Biomedicine 19, 255-263.

Schulte, R.F., Lange, T., Beck, J., Meier, D., Boesiger, P., 2006. Improved two-dimensional J-resolved spectroscopy. NMR in Biomedicine 19, 264-270.

Slotboom, J., Boesch, C., Kreis, R., 1998. Versatile frequency domain fitting using time domain models and prior knowledge. Magnetic Resonance in Medicine 39, 899-911.

Snyder, J., Lange, T., 2012. GABA Detection *In Vivo*: J-Editing Via Homonuclear Polarization Transfer (JET). 20th Annual Meeting of the International Society of Magnetic Resonance in Medicine. International Society of Magnetic Resonance in Medicine, Melbourne, Australia, p. 1743.

Snyder, J., Wilman, A., 2010. Field strength dependence of PRESS timings for simultaneous detection of glutamate and glutamine from 1.5 to 7T. J Magn Reson 203, 66-72.

Soher, B.J., Young, K., Bernstein, A., Aygula, Z., Maudsley, A.A., 2007. GAVA: spectral simulation for in vivo MRS applications. J Magn Reson 185, 291-299.

Tchong Len, B., Ratiney, H., Cudalbu, C., Fenet, B., Allouche, A.R., Aubert-Frécon, M., van Ormondt, D., Graveron-Demilly, D., 2004. Quantitation of edited GABA signals in magnetic resonance spectroscopy. ProRISC 2004, 15th Annual Workshop on Circuits, Systems and Signal Processing of IEEE Benelux, Veldhoven (NL), pp. 311-316.

Thomas, M.A., Hattori, N., Umeda, M., Sawada, T., Naruse, S., 2003. Evaluation of two-dimensional L-COSY and JPRESS using a 3 T MRI scanner: from phantoms to human brain in vivo. NMR in Biomedicine 16, 245-251.

Thomas, M.A., Lange, T., Velan, S.S., Nagarajan, R., Raman, S., Gomez, A., Margolis, D., Swart, S., Raylman, R.R., Schulte, R.F., Boesiger, P., 2008. Two-dimensional MR spectroscopy of healthy and cancerous prostates in vivo. Magn Reson Mater Phy 21, 443-458.

Thomas, M.A., Ryner, L.N., Mehta, M.P., Turski, P.A., Sorenson, J.A., 1996. Localized 2D J-resolved 1H MR spectroscopy of human brain tumors in vivo. Journal of Magnetic Resonance Imaging 6, 453-459.

Thomas, M.A., Yue, K., Binesh, N., Davanzo, P., Kumar, A., Siegel, B., Frye, M., Curran, J., Lufkin, R., Martin, P., Guze, B., 2001. Localized two-dimensional shift correlated MR spectroscopy of human brain. Magnetic Resonance in Medicine 46, 58-67.

Vallisneri, M., 2008. Use and abuse of the Fisher information matrix in the assessment of gravitational-wave parameter-estimation prospects. Physical Review D 77, 042001.

van Ormondt, D., de Beer, R., Marien, A.J.H., den Hollander, J.A., Luyten, P.R., Vermeulen, J.W.A.H., 1990. 2D approach to quantitation of inversion-recovery data. Journal of Magnetic Resonance 88, 652-659.

Vanhamme, L., van Huffel, S., Van Hecke, P., van Ormondt, D., 1999. Time-domain quantification of series of biomedical magnetic resonance spectroscopy signals. J Magn Reson. 140, 120-130.

Wilson, M., Reynolds, G., Kauppinen, R.A., Arvanitis, T.N., Peet, A.C., 2011. A constrained least-squares approach to the automated quantitation of in vivo (1)H magnetic resonance spectroscopy data. Magnetic Resonance in Medicine 65, 1-12.

Table 1

Table 1.

optimized for	**CRB** [in % of values for reference experiment]			
	GABA	Glu	Gln	GSH
×	100	100	100	100
GABA	**96**	97	95	97
Glu	113	**84**	92	102
Gln	106	90	**87**	101
GSH	100	95	90	**95**
GABA	**92**	115	101	100
Glu	121	**80**	90	101
Gln	106	86	**87**	98
GSH	96	105	93	**94**
GABA & Glu	**93**	**101**	96	97

Figure 1
Click here to download 9. Figure: FIG1.pdf

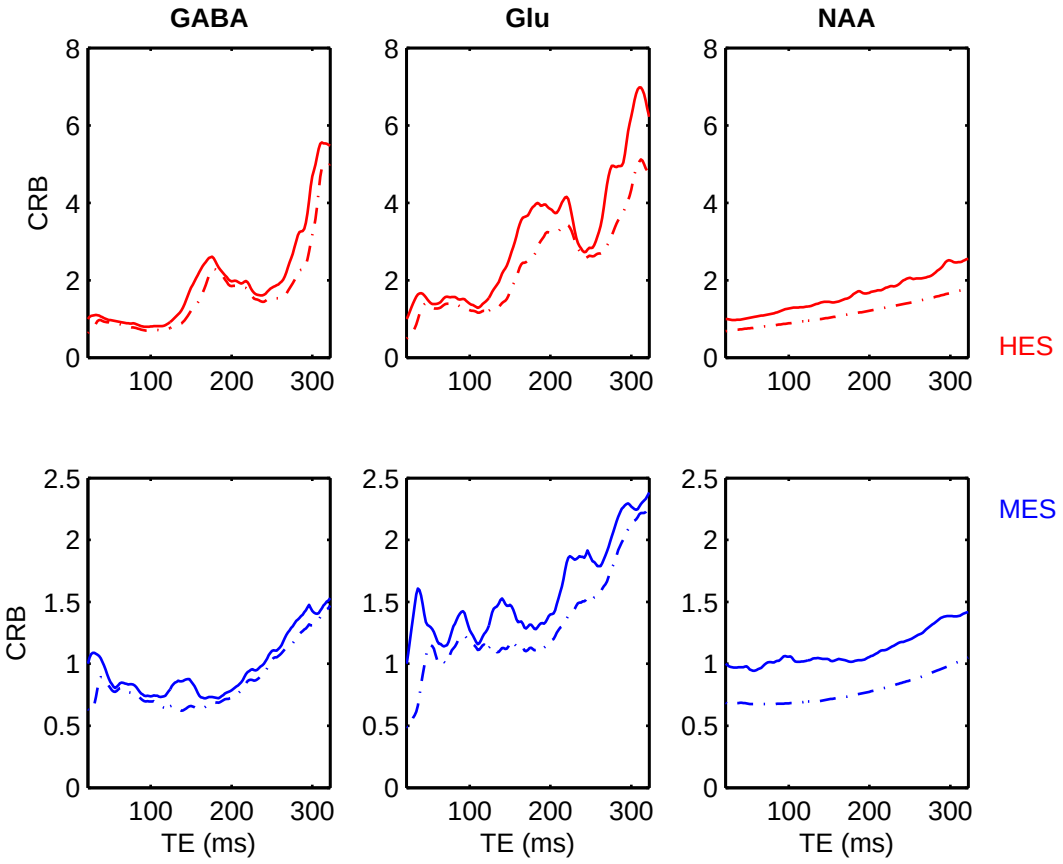

Figure 2

Click here to download 9. Figure: FIG2.pdf

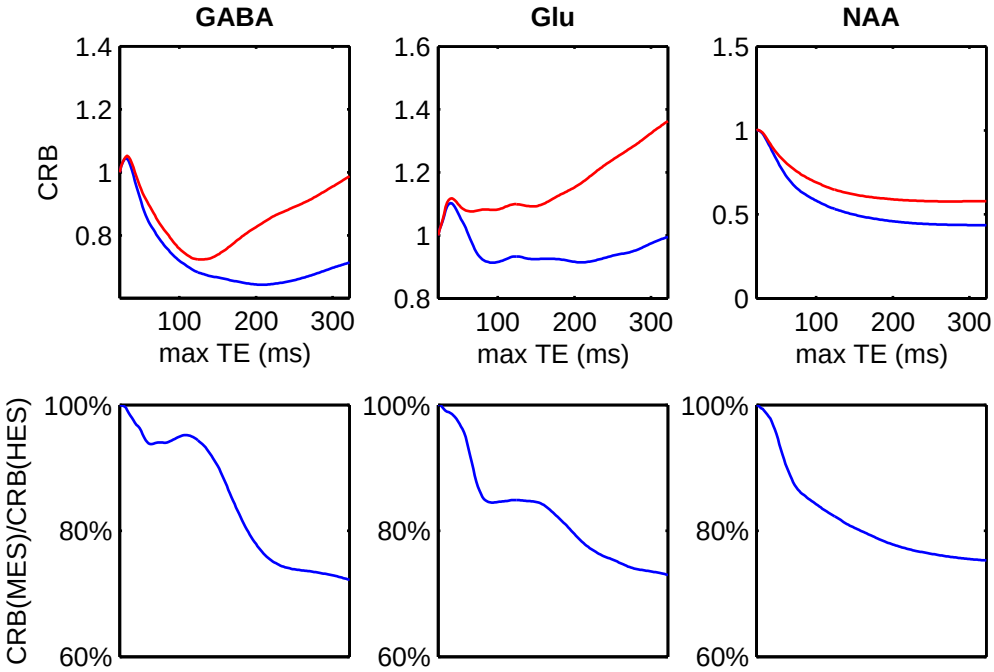

Figure 3

Click here to download 9. Figure: FIG3.pdf

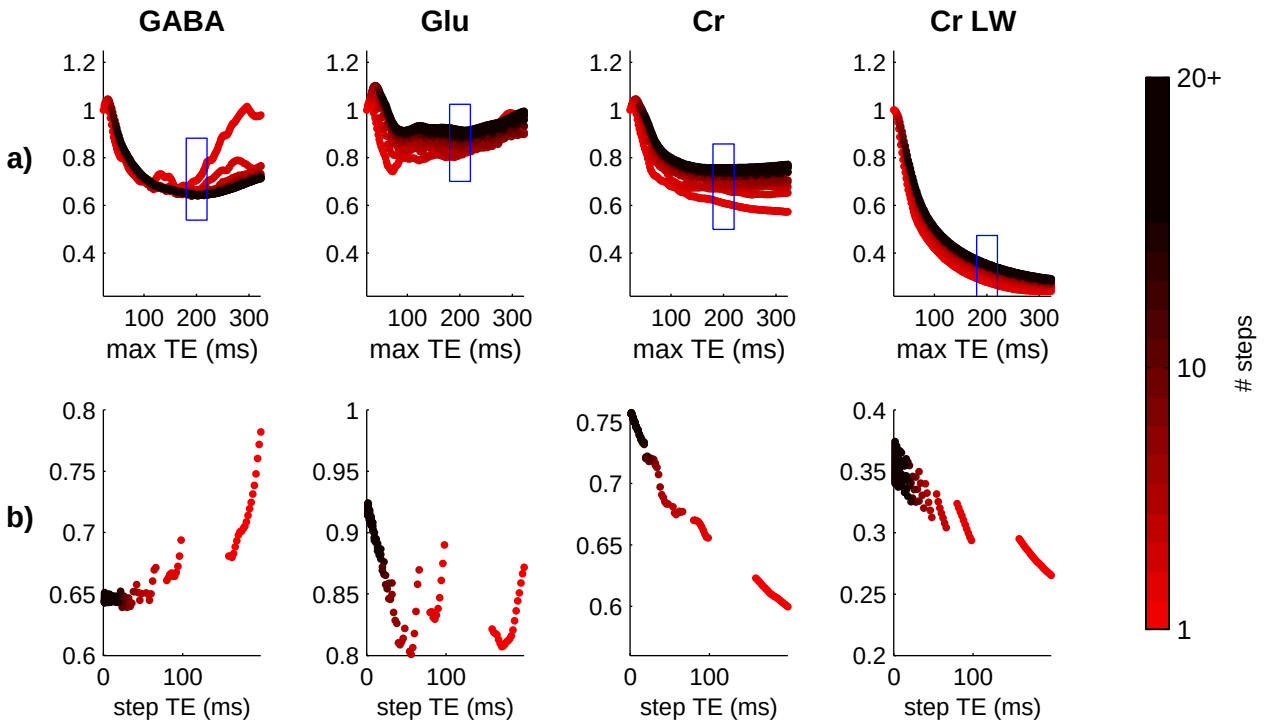

Figure 4

Click here to download 9. Figure: FIG4.pptx

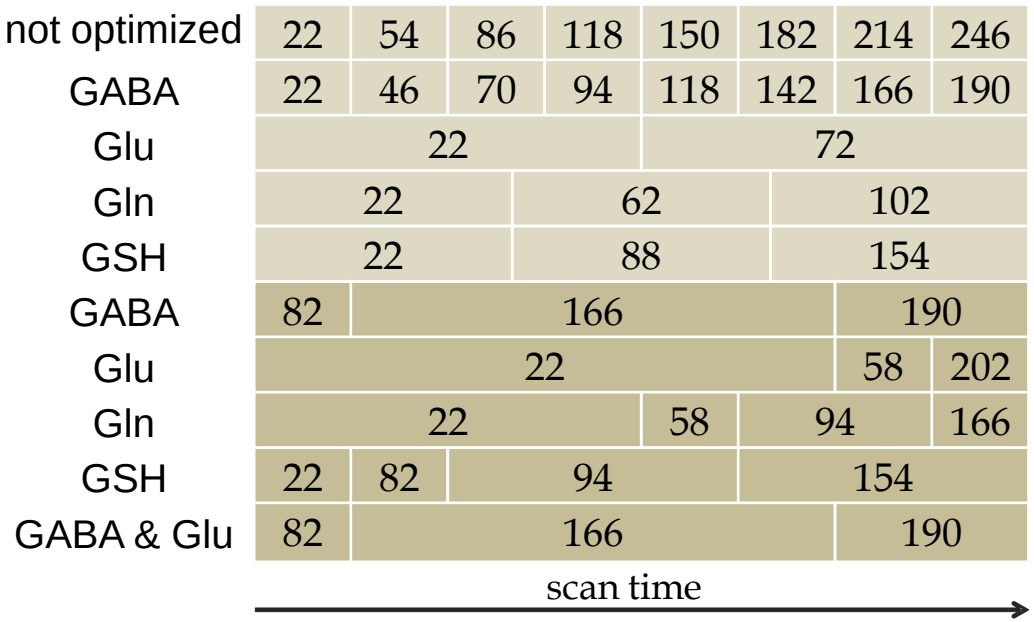

Figure 5
Click here to download 9. Figure: FIG5.pdf

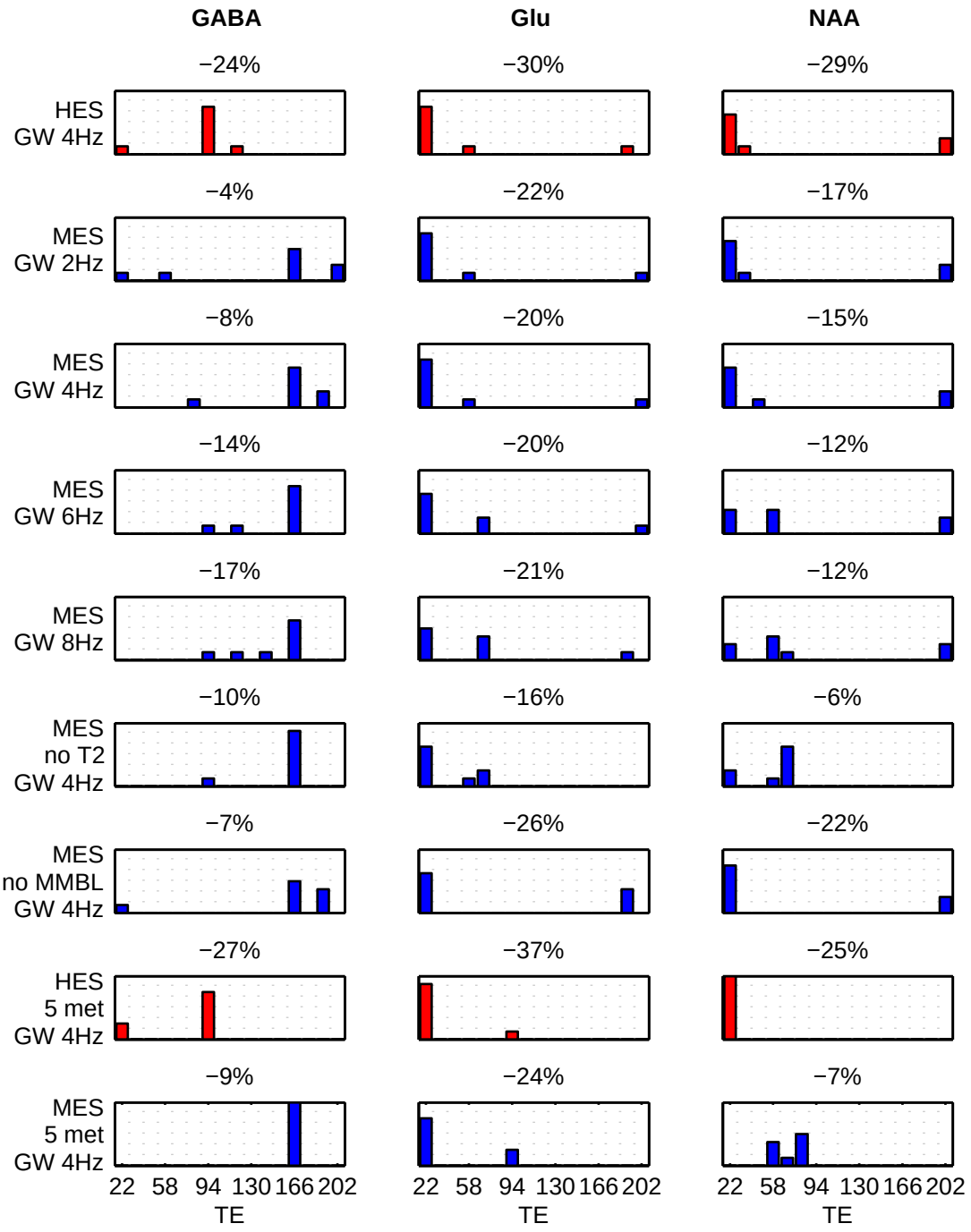

Figure 6

Click here to download 9. Figure: FIG6.pptx

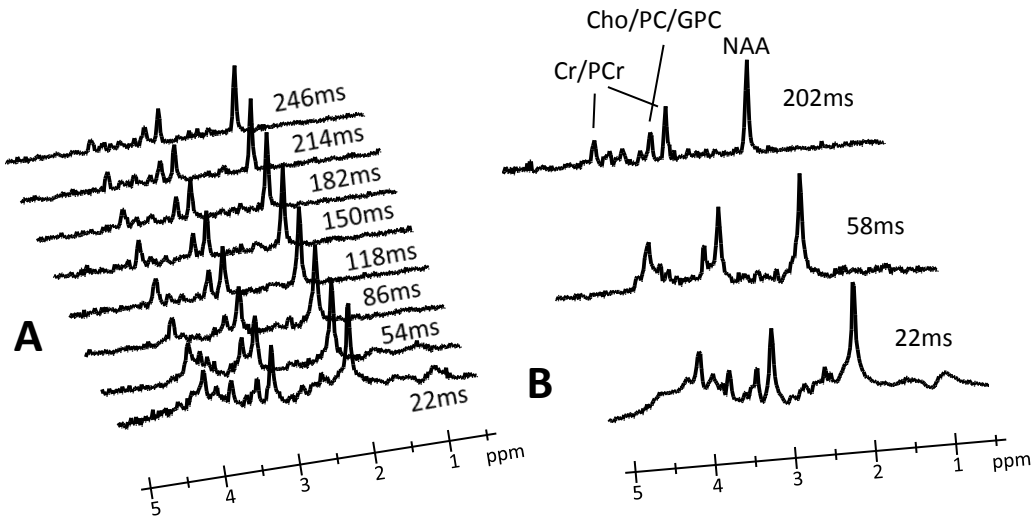

Figure 7

Click here to download 9. Figure: FIG7.pdf

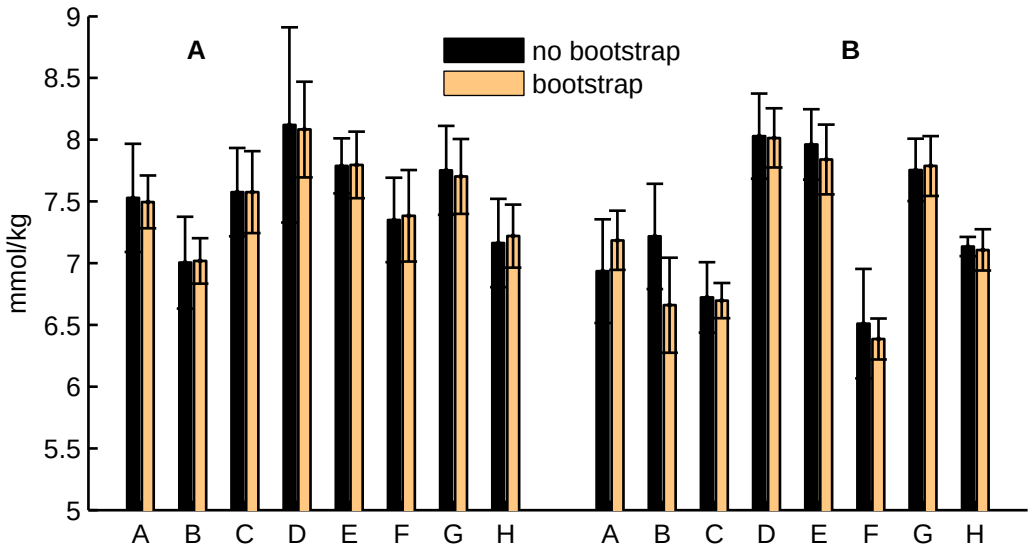

Inline Supplementary Figure ES1

Click here to download Inline Supplementary Table: FIG3b.pdf

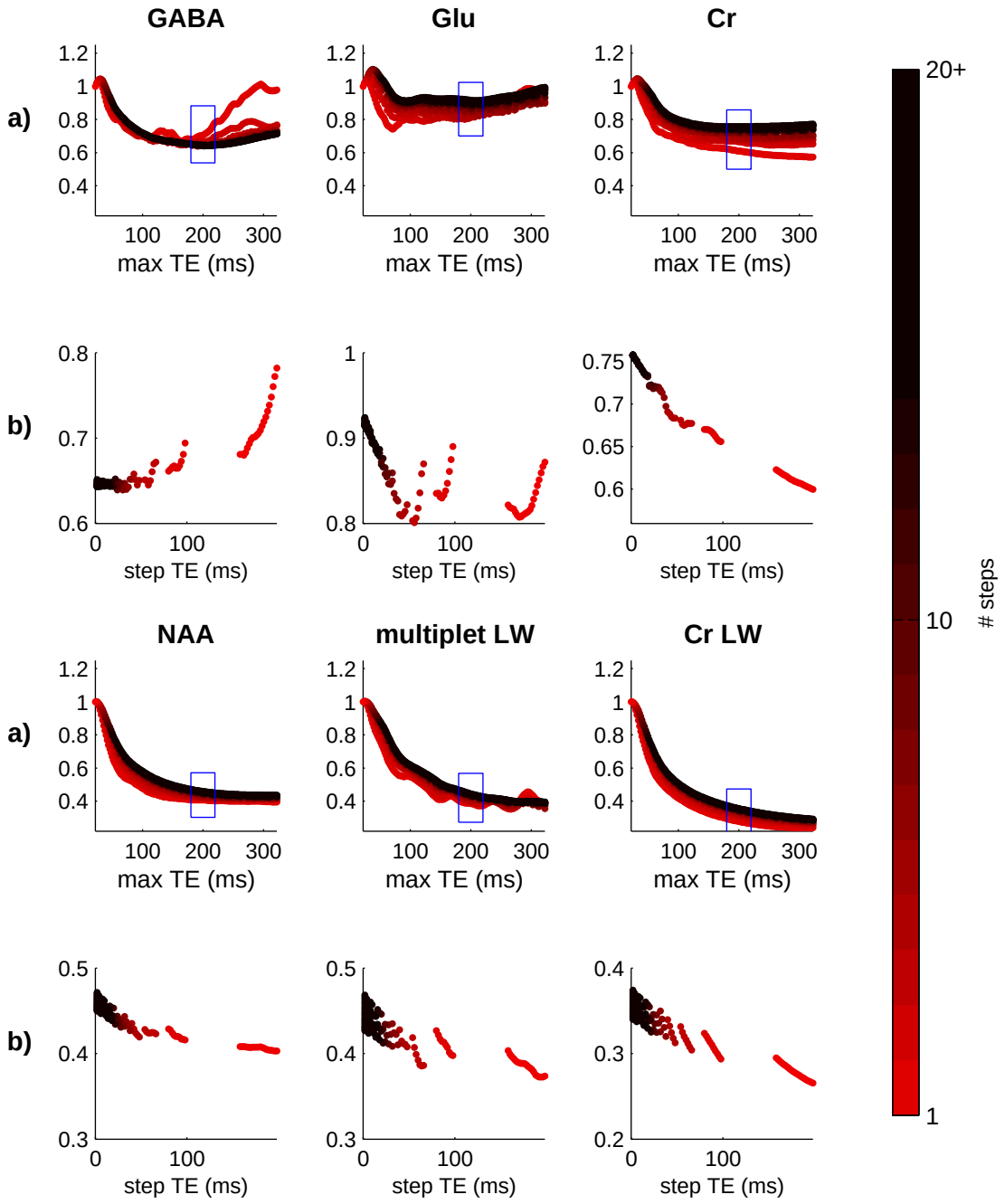

Inline Supplementary Figure ES2

Click here to download Inline Supplementary Table: FIG_ES2.pptx

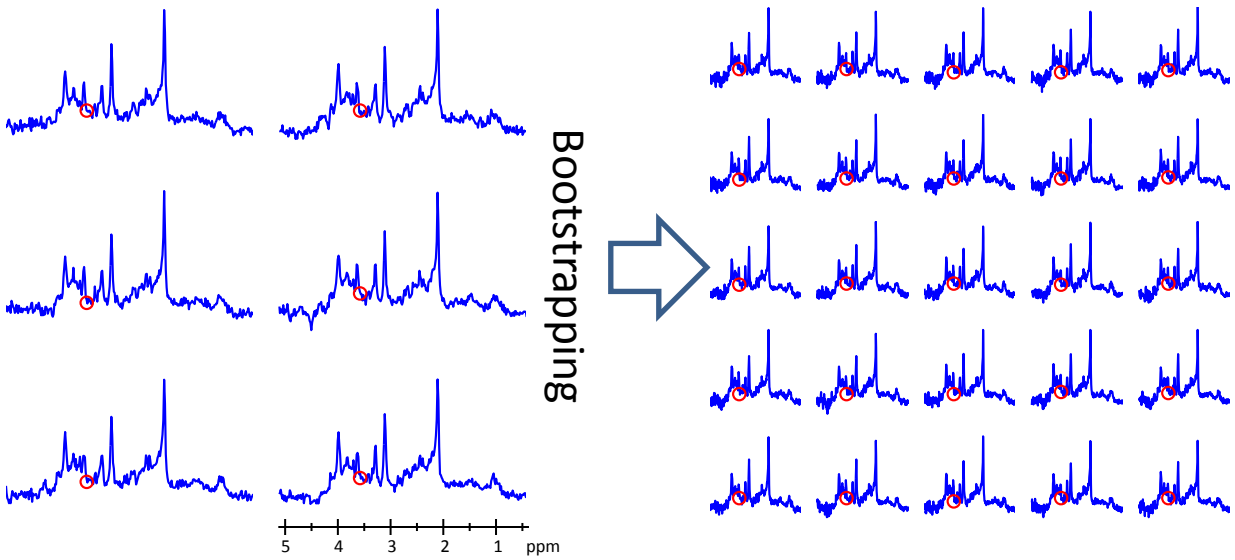

Inline electronic supplement

P. Mathematical Proofs

P1. Lower bound for diagonal elements of the inverse of a positive-definite matrix

The inverse of the square root of the diagonal elements of the Fisher matrix provide a lower bound to the respective CRB.

Statement:

For any positive definite matrix F, the following holds:

$$(F_{kk})^{-1} \leq (F^{-1})_{kk} \qquad \textit{[Eq. A1]}$$

Proof:

Let $F = U \cdot \Lambda \cdot U^t$ be the eigenvalue decomposition of F, where U is the unitary matrix ($U \cdot U^t = U^t \cdot U = \mathbb{I}$) whose columns are the normalized eigenvectors (orthogonalized for eigenvalues of multiplicity greater than 1) and Λ is the diagonal matrix whose main diagonal contains the corresponding eigenvalues $\Lambda_{ll} = \lambda_l > 0$.

It follows that $F^{-1} = U \cdot \Lambda^{-1} \cdot U^t$.

Thus we conclude that

$$
\begin{aligned}
(F_{kk}) \cdot (F^{-1})_{kk} &= \left(\sum_l \lambda_l \, |U_{kl}|^2\right)\left(\sum_m \frac{1}{\lambda_m} |U_{km}|^2\right) = \sum_{lm} \frac{\lambda_l}{\lambda_m} \cdot |U_{kl}|^2 \cdot |U_{km}|^2 \\
&= \frac{1}{2} \sum_{lm} \left(\frac{\lambda_l}{\lambda_m} + \frac{\lambda_m}{\lambda_l}\right) |U_{kl}|^2 \cdot |U_{km}|^2 \geq \frac{1}{2} \sum_{lm} 2 \, |U_{kl}|^2 \cdot |U_{km}|^2 \\
&= \left(\sum_l |U_{kl}|^2\right)\left(\sum_m |U_{km}|^2\right) = 1
\end{aligned}
$$

Here we used that $x + \frac{1}{x} \geq 2$ for any $x > 0$.

P2. CRB cannot be decreased by neglecting information

Increasing the number of data points is reflected in adding rows to the matrix of partial derivatives D and thus adding a positive-semidefinite matrix to the original (positive-definite) information matrix, which leads to decreased or unchanged values on the diagonal of the inverse (and thus CRB) . Conversely, neglecting information may lead to an increase in CRB, but never to a decrease.

Statement:

For a positive-definite matrix F and a positive-semidefinite matrix G it holds that

$$[(F+G)^{-1}]_{kk} \leq (F^{-1})_{kk}, \qquad \textit{[Eq. A2]}$$

with equality if and only if all eigenvalues of F are zero (F is nilpotent).

Proof:

Let $F = U \cdot \Lambda \cdot U^t$ be the eigenvalue decomposition of F, where U is the unitary matrix whose columns are the normalized eigenvectors and Λ is the diagonal matrix whose main diagonal contains the corresponding eigenvalues $\Lambda_{ll} = \lambda_l > 0$.

Defining $B \doteq \Lambda^{-1/2} \cdot U^t$, and b_k as the k-th column vector of B, we can write

$F^{-1} = U \cdot \Lambda^{-1} \cdot U^t = B^t \cdot B$, and thus

$(F^{-1})_{kk} = b_k^t \cdot b_k = |b_k|^2$.

Further, we define $\tilde{G}$ by $G = U \cdot \tilde{G} \cdot U^t$ and write

$$F + G = U \cdot \left(\Lambda + \tilde{G}\right) \cdot U^t = U \cdot \Lambda^{1/2} \cdot \left(\mathbb{I} + \Lambda^{-1/2} \cdot \tilde{G} \cdot \Lambda^{-1/2}\right) \cdot \Lambda^{1/2} \cdot U^t$$
$$= U \cdot \Lambda^{1/2} \cdot (\mathbb{I} + V \cdot \Delta \cdot V^t) \cdot \Lambda^{1/2} \cdot U^t = U \cdot \Lambda^{1/2} \cdot V \cdot (\mathbb{I} + \Delta) \cdot V^t \cdot \Lambda^{1/2} \cdot U^t,$$

where we introduced the eigenvalue decomposition

$\Lambda^{-1/2} \cdot \tilde{G} \cdot \Lambda^{-1/2} = V \cdot \Delta \cdot V^t$, with $V \cdot V^t = V^t \cdot V = \mathbb{I}$ and

$\Delta_{ll} = \delta_l \geq 0$ (since G and thus $\Lambda^{-1/2} \cdot \tilde{G} \cdot \Lambda^{-1/2}$ are positive semi-definite).

It follows that $(F + G)^{-1} = B^t \cdot A \cdot B$ with $A \doteq V \cdot (\mathbb{I} + \Delta)^{-1} \cdot V^t$,

and hence the diagonal elements can be written as

$$[(F + G)^{-1}]_{kk} = b_k^t \cdot A \cdot b_k.$$

A is a Hermitian matrix with eigenvalues ${}^{1}/_{(1 + \delta_l)} \leq 1$.

Expressing b_k in the basis of eigenvectors of A, i.e. $b_k = V c_k$ and thus $|c_k|^2 = |b_k|^2$, yields:

$$[(F + G)^{-1}]_{kk} = b_k^t \cdot A \cdot b_k = c_k^t \cdot V^t V \cdot (\mathbb{I} + \Delta)^{-1} \cdot V^t V \cdot c_k = c_k^t \cdot (\mathbb{I} + \Delta)^{-1} \cdot c_k$$
$$\leq \max_l \left({}^{1}/_{(1 + \delta_l)}\right) \cdot |c_k|^2 \leq |c_k|^2 = |b_k|^2 = (F^{-1})_{kk},$$

as required.

F: Figures

Figure ES1:

Cramér- Rao minimum variance bounds for conventional 2DJ experiments as function of maximum TE and TE sampling density. Row a) shows relative CRB values of all sampled 2DJ experiments as a function of the maximal TE, while row b) zooms into the subset of experiments with maximum TE between 180 and 220 ms (blue rectangle in the upper row) and shows these selected CRBs as a function of TE step size (relative scaling for CRBs as in Fig. 1). In this extension of Fig. 3 CRBs for four metabolite areas and two linewidth parameters are shown. The data are color-coded depending on the number of steps: darker colored dots refer to finely-sampled 2DJ, brighter dots to a coarser sampling. Example: experiment consisting of TEs 22, 36, 50 ms → max TE = 50ms, TE step = 14 ms, number of steps = 3.

Figure ES2:

Single spectra from 2DJ datasets illustrating the bootstrapping method used to extend the number of repeated experiments to determine the coefficient of variance for fitted Glu when comparing conventional with optimized 2DJ. On the left the spectra with TE 22 ms from each of the repeated generalized 2DJ spectra (c.f. Fig. 7 B) is plotted for one subject, while on the right, the 25 corresponding spectra obtained by bootstrapping are depicted, where each data point (for all TEs) was randomly picked from one of the six original 2D spectra